

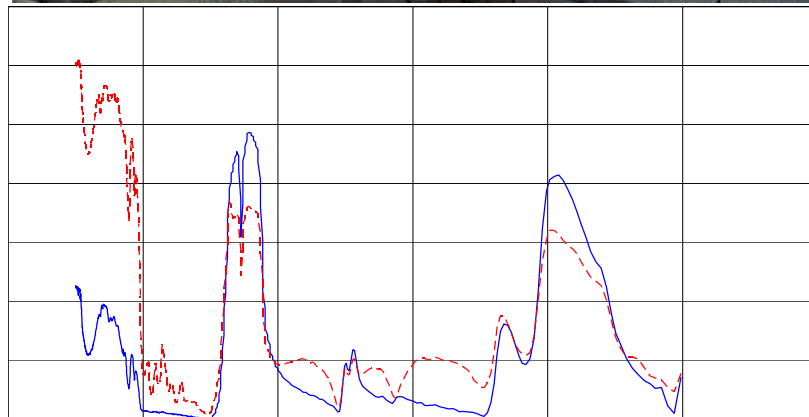


US Army Corps
of Engineers®
Engineer Research and
Development Center

Analysis of Long Wave Infrared (LWIR) Soil Data to Predict Reflectance Response

Janet E. Simms, Ernest S. Berney IV, Danny W. Harrelson,
Maureen K. Corcoran, and Ray M. Castellane

August 2009



Analysis of Long Wave Infrared (LWIR) Soil Data to Predict Reflectance Response

Janet E. Simms, Ernest S. Berney IV, Danny W. Harrelson,
Maureen K. Corcoran, and Ray M. Castellane

*Geotechnical and Structures Laboratory
U.S. Army Engineer Research and Development Center
3909 Halls Ferry Road
Vicksburg, MS 39180-6199*

Final report

Approved for public release; distribution is unlimited.

Abstract: The spectral response of quartz is a phenomenon of interest to countermine technologies because of suspected disruption in spectral signature from disturbed soil during emplacement of landmines in the subsurface. The research was divided into two: data analysis using spectral information from the Advanced Spaceborne Thermal Emission and Reflection (ASTER) spectral library and a laboratory study using a Fourier transform infrared (FTIR) spectrometer.

Spectral and mineralogical data for five major soil orders (Alfisols, Aridisols, Entisols, Mollisols, and Inceptisols) were acquired from the spectral library. Using these data, the relationship of the percentage of reflectance around the 8.2- μm quartz peak to the percentage of quartz in a soil was used to develop a linear regression model. The equations from this model predict the expected quartz peak reflectance for a soil of given quartz percentage. The predictive equations determined from the ASTER database can be modified based on quartz species and grain size to enable better prediction of expected reflectance from natural soils.

The FTIR system was used to measure the spectral response of different forms of quartz, clays, and quartz-clay mixtures. The spectral results revealed that different species of quartz exhibit different reflectance spectra, suggesting that the quartz reflectance response of a given soil type will vary depending on its impurities and depositional history. Grain-size fraction plays an important role in influencing the magnitude of reflectance. From the pure quartz studied, as grain size decreased from particle diameters of 1180 μm to less than 300 μm , FTIR reflectance increased according to a logarithmic relationship.

DISCLAIMER: The contents of this report are not to be used for advertising, publication, or promotional purposes. Citation of trade names does not constitute an official endorsement or approval of the use of such commercial products. All product names and trademarks cited are the property of their respective owners. The findings of this report are not to be construed as an official Department of the Army position unless so designated by other authorized documents.

DESTROY THIS REPORT WHEN NO LONGER NEEDED. DO NOT RETURN IT TO THE ORIGINATOR.

Contents

Figures and Tables	iv
Preface	v
Summary	vi
1 Introduction	1
Reststrahlen	1
Geologic influences.....	2
Approach.....	4
2 ASTER Data Analysis	6
Soil spectra data analysis.....	6
Influence of impurities	11
Influence of quartz content	12
3 Laboratory Study	16
Purpose.....	16
Approach.....	16
Influence of grain size.....	17
Influence of quartz species	19
Influence of fines content.....	19
4 Conclusions and Recommendations	22
Conclusions	22
Recommendations	23
References	25
Appendix A: Summary of Soil Data	27
Report Documentation Page	

Figures and Tables

Figures

Figure 1. Location of the major soil orders throughout the world (USDA–NRCS 1999).	7
Figure 2. Location of the major soil orders throughout the United States (USDA–NRCS 1999).....	8
Figure 3. Distribution of the major soil classes in the world and United States (USDA–NRCS 1999).....	9
Figure 4. Percentage of peak reflectance at the 8.2- μ m wavelength related to the percentage of clay in soil.	9
Figure 5. Percentage of peak reflectance at the 8.2- μ m wavelength related to the percentage of silt in the soil.	10
Figure 6. Percentage of peak reflectance at the 8.2- μ m wavelength related to the percentage of sand in the soil.....	10
Figure 7. Percentage of peak reflectance at the 8.2- μ m wavelength related to grain size for pure quartz and different quartz varieties (ASTER 1999).	12
Figure 8. Linear fit to the combined ASTER soils data set. Percentage of peak reflectance at the 8.2- μ m wavelength related to the percentage of quartz present in the soil sample.....	13
Figure 9. Linear fits of percentage of peak reflectance in Alfisols at the 8.2- μ m wavelength related to the percentage of quartz present in the soil sample.	14
Figure 10. Linear fits of percentage of peak reflectance in Ardisols at the 8.2- μ m wavelength related to the percentage of quartz present in the soil sample.	14
Figure 11. Linear fits of percentage of peak reflectance in Mollisols at the 8.2- μ m wavelength related to the percentage of quartz present in the soil sample.	15
Figure 12. Linear fits of percentage of peak reflectance in Inceptisols at the 8.2- μ m wavelength related to the percentage of quartz present in the soil sample.	15
Figure 13. Nicolet 750 Fourier Transform Infrared Spectrometer.....	16
Figure 14. Spectra of coarser (50+) and finer (50-) grained quartz material.	18
Figure 15. Reflectance for varying grain-size fractions for Hot Springs quartz.	18
Figure 16. Trend of reflectance (y) for Hot Springs quartz with grain-size fraction (x).	19
Figure 17. Comparison of spectra for three quartz species or three quartz species (coarser than No. 50 sieve).	20
Figure 18. Spectrum of pure montmorillonite sample.	20
Figure 19. Spectra of montmorillonite mixed with the three quartz species (50/50).	21

Tables

Table 1. Spectral region of typical quartz features (Kelch et al. 1999).....	2
Table 2. Relationships between percentage quartz content (x) to peak reflectance (y).	13
Table A1. Summary of soil data (ASTER Spectral Library).....	28

Preface

This report was prepared as part of the U.S. Army Engineer Research and Development Center's (ERDC) Countermine Phenomenology Program, which supports the mine detection sensor test and development programs of the U.S. Army Research, Development and Engineering Command, Communications and Electronics Research, Development and Engineering Center, Night Vision and Electronic Sensors Directorate (NVESD). The NVESD Technical Monitor for this effort was Dr. Tom Broach of the NVESD Mine Division, located at Fort Belvoir, VA. Bart Durst, ERDC Geotechnical and Structures Laboratory (GSL), Vicksburg, MS, was the manager of the Countermine Phenomenology Program.

Personnel of the ERDC GSL conducted the research, and this report was prepared by Dr. Janet E. Simms and Danny W. Harrelson, Geotechnical Engineering and Geosciences Branch (GEGB), and Ray M. Castellane III, Survivability Engineering Branch (SvEB), all of the Geosciences and Structures Division (GSD); Dr. Maureen K. Corcoran, Office of the Technical Directors; and Dr. Ernest S. Berney IV, Airfields and Pavements Branch (APB), Engineering Systems and Materials Division (ESMD). Dr. Lillian D. Wakeley, ESMD Research Group, also contributed to this report.

Work was conducted under the supervision of Dr. Gary L. Anderton, Chief, APB; Dr. Monte L. Pearson, Chief, GEGB; James L. Davis, Chief, SvEB; Dr. Larry N. Lynch, Chief, ESMD; Dr. Robert L. Hall, Chief, GSD; and Dr. William P. Grogan, Deputy Director, GSL; and Dr. David W. Pittman, Director, GSL.

COL Gary E. Johnston was Commander and Executive Director of ERDC. Dr. James R. Houston was Director.

Recommended changes for improving this publication in content and/or format should be submitted on DA Form 2028 (Recommended Changes to Publications and Blank Forms) and forwarded to Headquarters, U.S. Army Corps of Engineers, ATTN: CECW-EW, Kingman Building, Room 321, 7701 Telegraph Road, Alexandria, VA 22315.

Summary

This report describes development of a preliminary method to predict the long-wave infrared (LWIR) reflectance response near the 8.2- μm quartz peak for a variety of soil types, in support of research on countermine technology. The 8.2- μm quartz peak represents a specific reststrahlen band of spectral reflectance. Soil disturbance, such as landmine emplacement, can disrupt the reflectance. The research is divided into two studies: data analysis from an existing spectral library and laboratory analysis using a Fourier transform infrared (FTIR) system.

Spectral and mineralogical data for five major soil orders (Alfisols, Aridisols, Entisols, Mollisols, and Inceptisols) were acquired from the Advanced Spaceborne Thermal Emission and Reflection (ASTER) spectral library. The library is a compilation of approximately 2000 spectra of natural and manmade materials from three spectral libraries: the John Hopkins University Spectral Library, the Jet Propulsion Laboratory Spectral Library, and the U.S. Geological Survey Spectral Library. The collective library is maintained by the Jet Propulsion Laboratory, California Institute of Technology. Data relating the percentage of reflectance around the 8.2- μm quartz peak to the percentage of quartz in a soil were used to fit linear equations. Each soil type was plotted individually and then combined into one data set. These relationships allowed prediction of an expected 8.2- μm quartz peak reflectance for a soil of given quartz percentage. An average expression for the combined data set is presented when the user encounters a situation in which no knowledge of the soil order, mineral content, or impurities is available. This is given in Equation 1, which defines the expected peak reflectance for the native soil with knowledge of the quartz content.

$$\text{Reflectance (\%)} = 0.1595 * \text{Quartz content (\%)} \quad (1)$$

A laboratory was used to measure the spectral reflectance response of different forms of quartz, clays, and quartz-clay mixtures.

The reststrahlen response is also dependent on the type of quartz, impurities in the quartz grains, and the grain-size properties. The FTIR measurements revealed that different species of quartz exhibit different

spectra, suggesting that the quartz reflectance response of a given soil type within the LWIR waveband will vary depending on its parent material. Observed changes in peak reflectance increased by as much as 2.5 times the pure quartz reflectance. The ASTER dataset showed that impurities in quartz can alter the magnitude of the peak reflectance by a factor of as much as 2.5 as well. Therefore, with greater knowledge of the quartz origins, the reflectance magnitude of Equation 1 can be modified.

The FTIR study also explored the role of the grain-size fraction in determining the magnitude of reflectance. For a pure quartz sample, as the grain size decreased from particle diameters of 1180 μm to less than 300 μm , the spectral reflectance increased according to a logarithmic relationship given in Equation 2. Previous work suggests that reflectance increases with increasing grain size. However, these studies (Lyon 1964; Salisbury and Wald 1985) demonstrated this relationship only for soils of particle diameters less than 500 μm , and usually for the fraction less than 100 μm .

$$\text{Reflectance (\%)} = -3.656 \ln(\text{grain size in } \mu\text{m}) + 28.438 \quad (2)$$

The findings presented in this report provide a means to approximate the expected reststrahlen signatures in the field for native soil if knowledge of grain size and mineralogy is adequate. This can then improve the ability to detect disturbed soil locations or other foreign bodies based on differences in reststrahlen signature.

Future studies should focus on the coarser grain-size fraction of quartz materials, as this is more typical of grain sizes found in terrestrial environments. Grain size coupled with quartz content should account for many of the corrections necessary to predict field reflectance for undisturbed soils. Moisture and density remain the variables still to be studied and should be included in any further test programs.

1 Introduction

The U.S. Army Engineer Research and Development Center (ERDC) supports the Countermine Phenomenology Program and the Night Vision and Electronic Sensors Directorate (NVESD) through the characterization of the near-surface environment surrounding a mine. Various ERDC work units have addressed the characteristics of disturbed soil following mine emplacement. An initial need identified by NVESD is a table of the expected reststrahlen contrast for a known mineralogical composition of soil. This report describes development of a preliminary method to predict the long-wave infrared (LWIR) reflectance response near the 8.2- μm quartz peak (reststrahlen band) for a variety of soil types.

Reststrahlen

The following explanation of the reststrahlen effect is taken from Korte and Röseler (2005):

The term reststrahlen was coined following the observation by H. Rubens (more than a century ago) that repeated reflection of an infrared beam at the surface of a given material suppresses radiation at all wavelengths except for certain spectral intervals. The measured intensity for these special intervals (the reststrahlen range) indicates a reflectance of up to 80% or even more, while the maximum reflectance due to infrared bands of dielectric materials are usually <10%. After four reflections, the intensity of the latter is reduced by a factor of 10^{-4} compared to the intensity of the incident radiation, while the light in the reststrahlen range can maintain 40% of its original intensity by the time it reaches the detector. Obviously, this contrast increases with the number of reflections and explains the observation made by Rubens and the term reststrahlen (residual rays) used to describe this spectral selection.

A disturbed sample is one in which the soil structure has been compromised. The spectral response in such an environment would signal a possible foreign object, such as a subsurface mine. As expected, chemical and elemental components of a mineral are important in interpreting such a response. However, it is essential to address the physical aspects as well. Kelch et al. (1999) identify four characteristics used to detect soil

disturbance as mineralogical composition, particle size, particle coating, and lignin and cellulose content. In this context, a thorough understanding of the subsurface environment and soil mineralogy is needed to associate and interpret the response of optical and hyperspectral (HSI) instruments.

Geologic influences

Quartz (SiO_2) is a major component of soils. In addition, most of the silica in the earth's crust occurs as the polymorph of α -quartz (Broekmans 2004). As described by Salisbury and D'Aria (1992), remote sensing aids in identifying quartz and other soil constituents. As a result, the influence of soil particle size on the spectral emission of the soil is better understood. Within these emissions spectra, quartz displays prominent reststrahlen bands of 8 to 14 μm in the atmospheric window (Salisbury and D'Aria 1992). However, variation exists within the emissions spectra that cannot easily be described and interpreted from the soil type.

Based on research by Salisbury et al. (1987), the emittance spectra are a complex function of both the absorption coefficient and the refractive index, which affects spectral band shapes and intensities to such an extent that transmittance spectra alone cannot be used to predict emissivity. Hamilton (2003) also notes that changes in the infrared spectral character of minerals are affected if the tested mineral is dominated by particles whose sizes approach or are smaller than the wavelength of observation, a behavior referred to as volume scattering. Taking this information into consideration, directional hemispherical reflectance spectra can be used to predict emissivity in the reststrahlen region (Salisbury et al. 1987; Nicodemus 1965).

Kelch et al. (1999) identified 16 spectral features that can be used to detect signatures of disturbed soils. Table 1 is a subset of these features that pertain to the reststrahlen bands.

Table 1. Spectral region of typical quartz features (Kelch et al. 1999).

Spectral Feature	Spectral Region	Required Resolution	No. of Bands
LWIR quartz reststrahlen bands	8 to 10 μm and 12.2 μm	200 nm 200 nm	HSI 1
LWIR fine quartz and clay modifications of quartz reststrahlen bands	8 to 10 μm and 12.3 μm	50 nm 50 nm	HSI 1
LWIR feldspar reststrahlen band	9 to 10 μm	100 nm	HSI

Previous research addresses the emissivity of soil types by focusing on the particle size of the mineral itself, specifically quartz. Lyon (1964) concluded through his research on lunar and planetary soils that a progressive reduction in particle size removes the major reststrahlen features. As expected, grain size affects mineral solubility because of its increasing surface area with diminishing grain size. Quartz solubility increases significantly at grain sizes below $\sim 0.1 \mu\text{m}$ due to an inflection point occurring in the particle's free Gibbs energy ΔG_f (Broekmans 2004). Although laboratory analyses easily provide particle-size distribution on collected field samples, the in situ soil properties are sometimes lost in laboratory preparation. Not as easily addressed are dust, clay fines, and organics (collectively referred to in this proposal as particle debris) and also other silica-bearing minerals, such as biotite and potassium feldspar, which may inhibit or distort the reststrahlen wavelength.

Lack of understanding the source interfering with the reststrahlen response limits the effectiveness of many studies. The problem appears broad in scope; however, by applying a geological interpretation, the source of reststrahlen interference can be uncovered. Previous research has focused on soil type and usually ignores the mineralogical assemblage of the soil. The best approach to identify material that inhibits or distorts the reststrahlen bands is a thorough study of the mineralogical component of the soil. Knowing the soil type alone will not provide the information needed to fully interpret the reststrahlen response.

A given depositional environment is consistent in mineralogical characteristics. For example, most beaches in coastal marine environments consist of well-rounded and well-sorted quartz. The grain size and shape is influenced by water and wave action. By contrast, quartz-rich deposits in a desert environment will include a wider variety of particle sizes and shapes, because of the action of wind with little or no water.

Weathering alters the reststrahlen response by either exposing larger surface grains by "washing" of fine surface particles or coating larger surface grains with finer particles. Accordingly, the time lapse between physical weathering events, and the timing of soil disturbance relative to rainfall events, will also contribute to variation of the reststrahlen response. A field study using a portable Fourier transform infrared (FTIR) spectrometer is required to adequately predict the effects of weathering

and elapsed time on reststrahlen contrast (Hook and Kahle 1996; Koh et al. 2006). A proposed second phase of this research is to field test the laboratory results with a portable FTIR system.

The crystal structure of a given mineral and its elemental composition indicate its parent material or origin. These mineralogical features are useful in identifying a depositional environment and conditions under which the mineral formed. Salisbury and D'Aria (1992) found that crystal structure affects spectral behavior. Although crystal structure is unique for each mineral, polymorphs of a mineral may exist that possess the same elemental composition but differ in the crystal structure. For example, nine polymorphs (also known as species) of quartz exist with the same elemental composition (SiO_2) although each has its own crystal structure (Broekmans 2004), and additional silica polymorphs remain to be studied. Therefore, information about both mineralogy and the elemental composition is needed to fully assess the reststrahlen effect.

Approach

This study focuses on the influence that mineral composition has on soil reflectance as a function of quartz species, grain size, and mineralogy. For simplicity, soil classification can be limited to the 12 major soil orders of the classification system defined by the U.S. Department of Agriculture (USDA) Natural Resources Conservation Service (USDA–NRCS 1999). In this system, soil orders are defined by the presence or absence of features that reflect soil-forming processes, rather than on engineering properties or grain-size distribution.

The 12 soil orders used in soil taxonomy of the USDA–NRCS (1999) are Alfisol, Andisol, Aridisol, Entisol, Gelisol, Histosol, Inceptisol, Mollisol, Oxisol, Spodosol, Ultisol, and Vertisol. The reststrahlen effect changes with geo-environmental factors and with time. To quantify the effect so that it can be tabulated, it is necessary to have a LWIR database that contains soil spectra measured over a variety of soil types, under varying weather conditions. The soils information must include grain-size analysis and quantitative mineralogy (percentage of each mineral present).

Several reports were provided by NVESD containing extensive spectral data accompanied by grain size information (ERIM International, Inc. 1999a, 1999b; MTL Systems, Inc. 1999; SAIC 1998). However, those reports addressed the soil mineralogy qualitatively and identified the

prominent minerals present in the soil, but did not provide the percentage of each mineral present in a given soil. Because these previous reports did not include quantitative mineralogical descriptions, they could not be used for predictive analysis in this study.

2 ASTER Data Analysis

Twelve major soil orders as defined by the NRCS have been mapped worldwide. The location and distribution of the major soil orders for both the world and the United States are shown in Figures 1 and 2, respectively.

To study soil influences, the ASTER (1999) spectral library was used. The library is a compilation of approximately 2000 spectra of natural and manmade materials from three spectral libraries: the John Hopkins University Spectral Library, the Jet Propulsion Laboratory Spectral Library, and the U.S. Geological Survey Spectral Library. The collective library is maintained by the Jet Propulsion Laboratory, California Institute of Technology. This library contains the spectral response of minerals from five major soil orders, including information on mineralogy and grain size. The five soil orders represented in the ASTER database are Alfisol, Aridisol, Entisol, Mollisol, and Inceptisol. These soils account for 63% of the soil coverage worldwide, and 71% of the United States (Figure 3).

Appendix A summarizes the soil information obtained from the ASTER database, including soil order, grain size information (percentages of sand, silt, and clay size particles), and mineralogy of the clay-size fraction and silt/sand-size fraction (labeled “clay” and “coarse,” respectively, in Appendix A). Only those datasets containing peak reflectance in the 8.2- μm bandwidth were used in the following analyses (reflectance is not shown in Appendix A). No indication of gravel content was noted in the ASTER database. The mineralogy and quartz content of each soil order were correlated with the spectral analysis signatures to identify trends characteristic of each soil order.

Soil spectra data analysis

In the following discussion, the terms clay, silt, and sand refer to the USDA texture class designation (USDA–NRCS 1993; 2002). The peak reflectance near the 8.2- μm wavelength was obtained from the ASTER spectral data file for each soil and plotted against the percentage of clay, silt, and sand comprising the soil (Figures 4, 5, and 6). Exponential trend lines are placed on each of the figures to illustrate the typical change in reststrahlen associated with the presence of ever-increasing percentages of each soil fraction. These are not intended for prediction purposes.

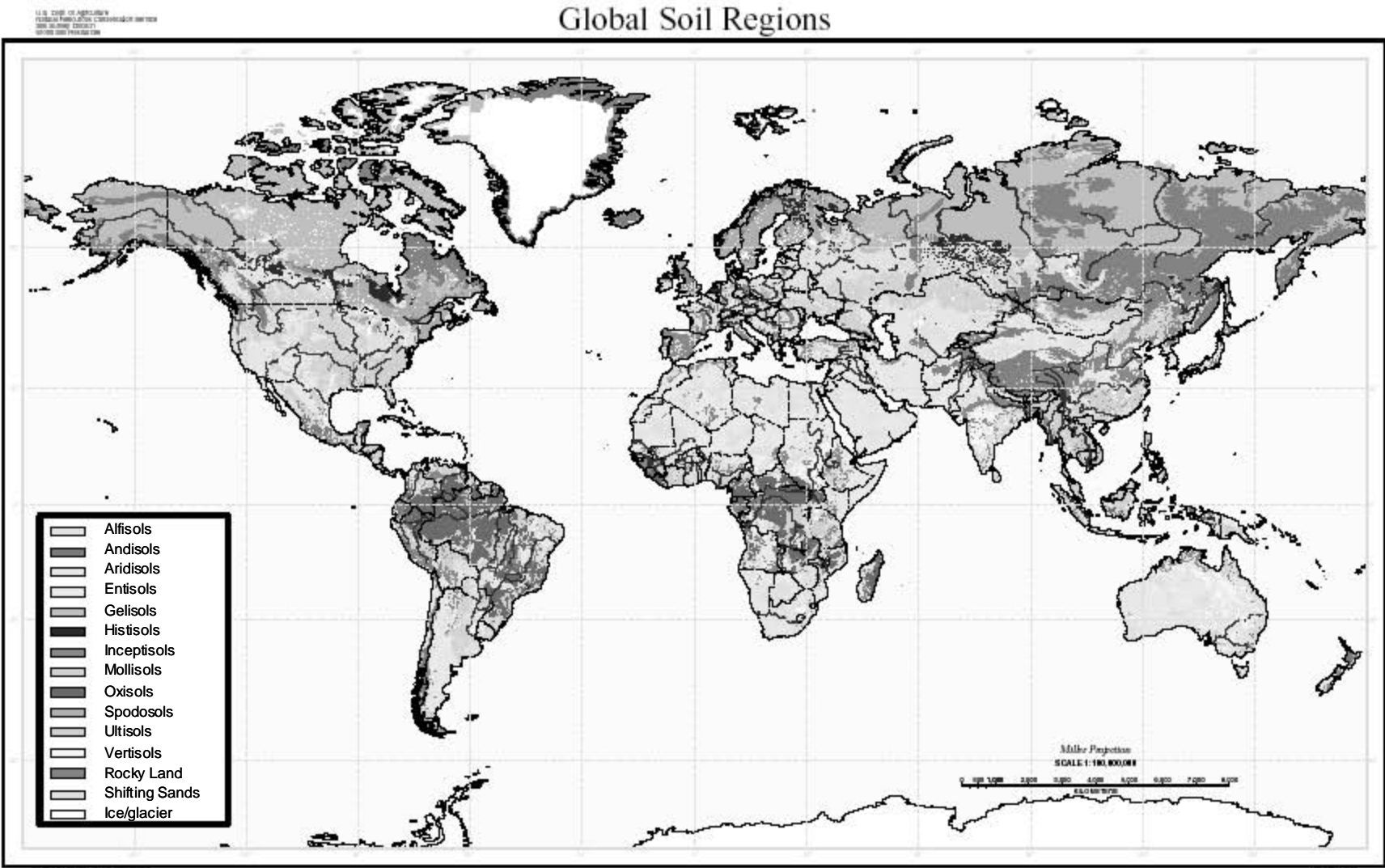


Figure 1. Location of the major soil orders throughout the world (USDA-NRCS 1999).

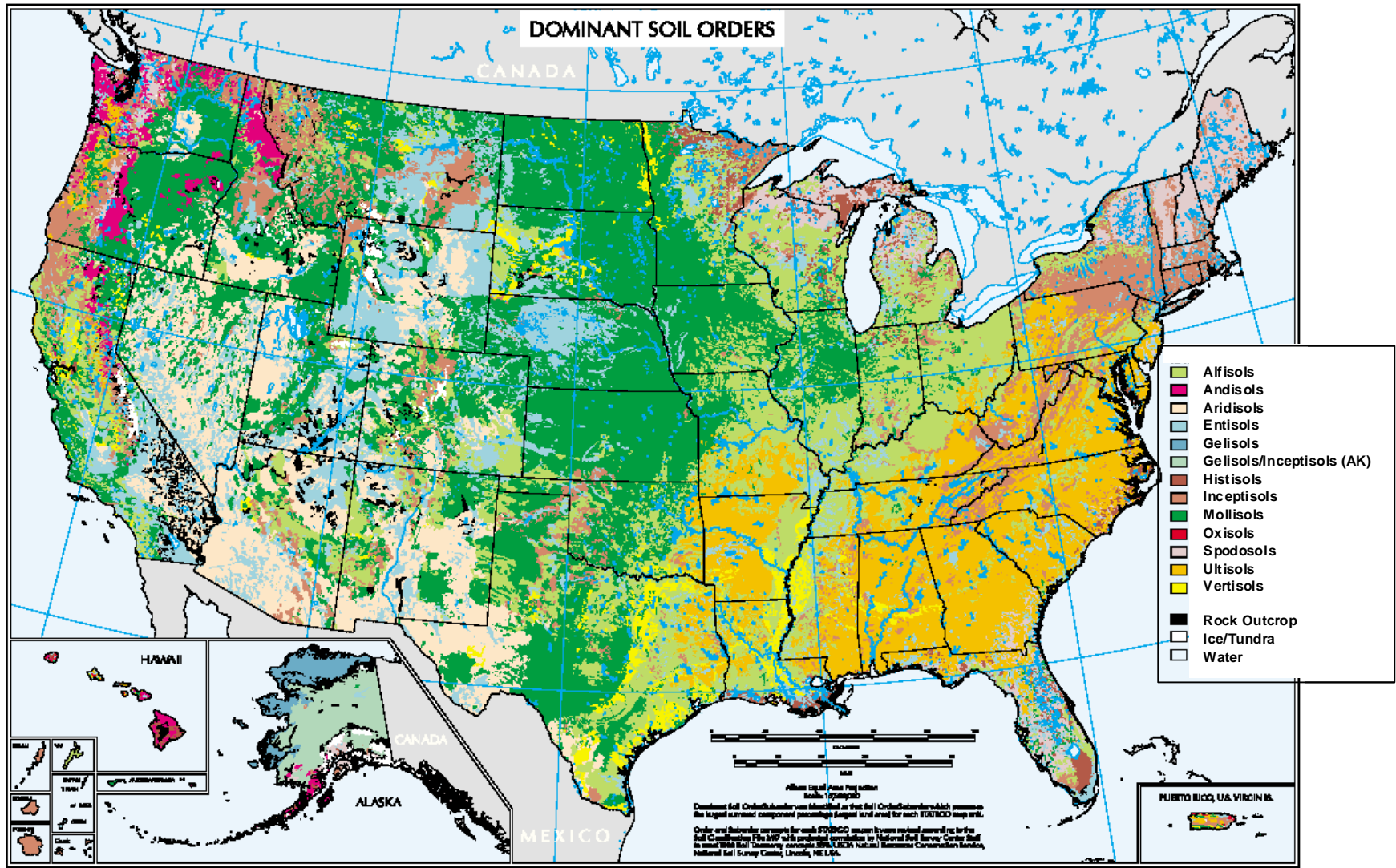


Figure 2. Location of the major soil orders throughout the United States (USDA-NRCS 1999).

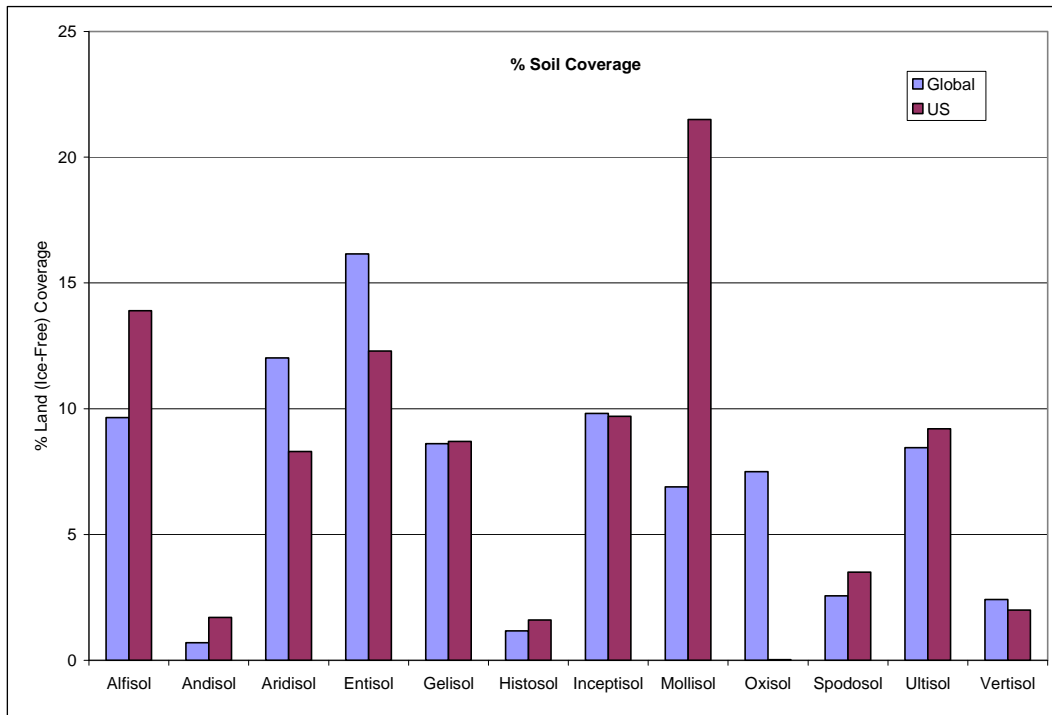


Figure 3. Distribution of the major soil classes in the world and United States (USDA-NRCS 1999).

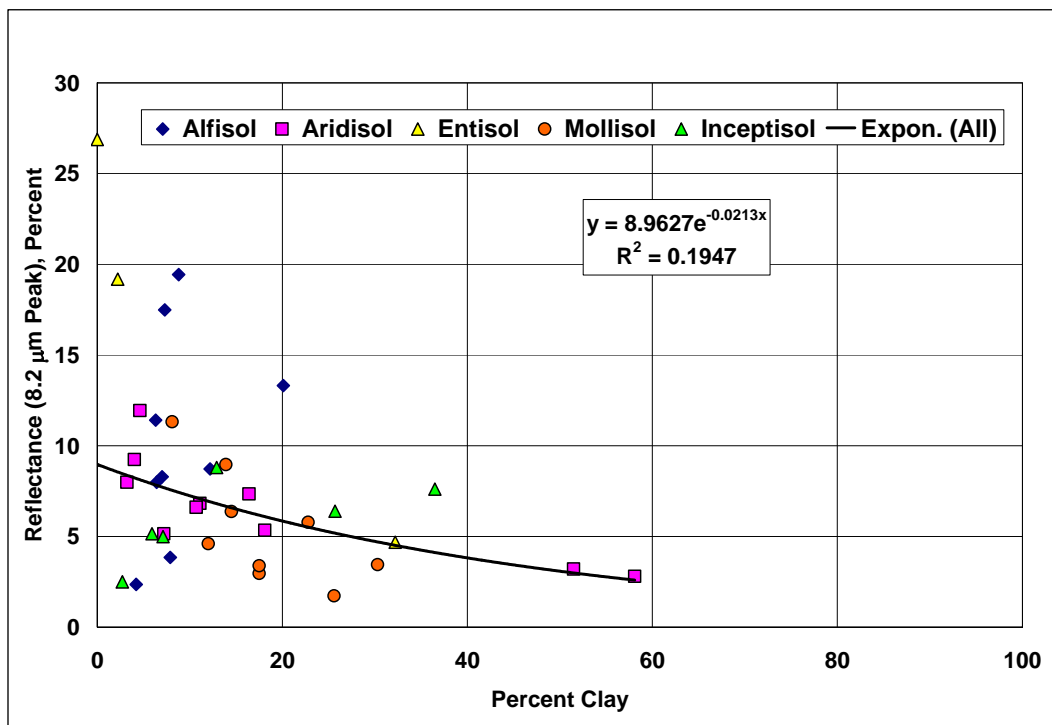


Figure 4. Percentage of peak reflectance at the 8.2-μm wavelength related to the percentage of clay in soil.

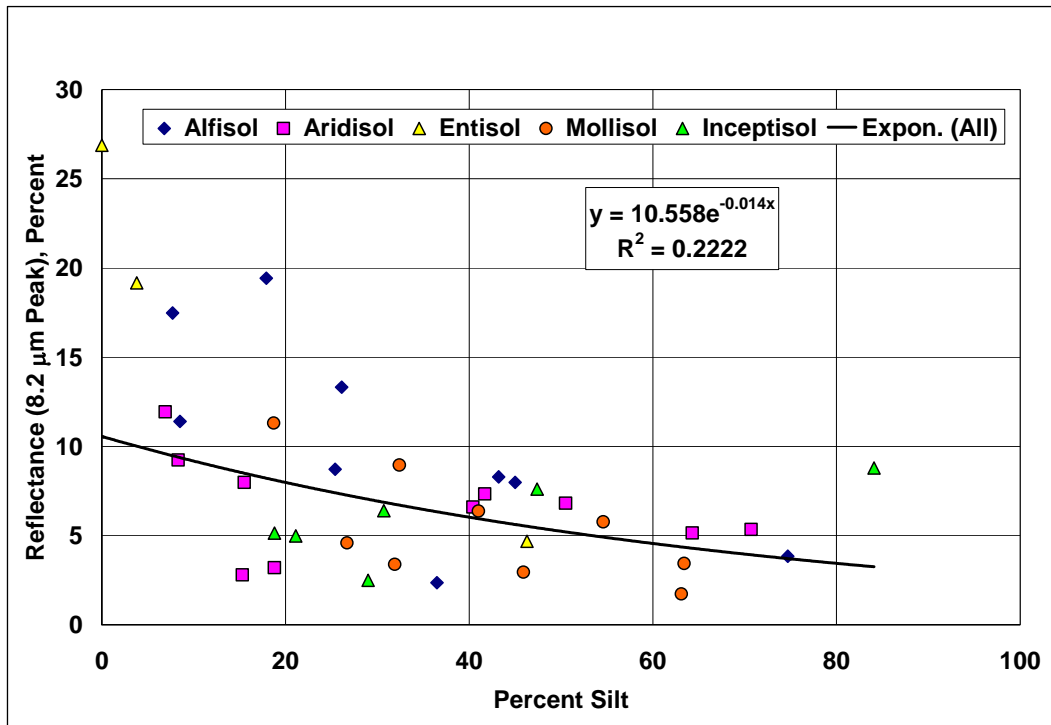


Figure 5. Percentage of peak reflectance at the 8.2-μm wavelength related to the percentage of silt in the soil.

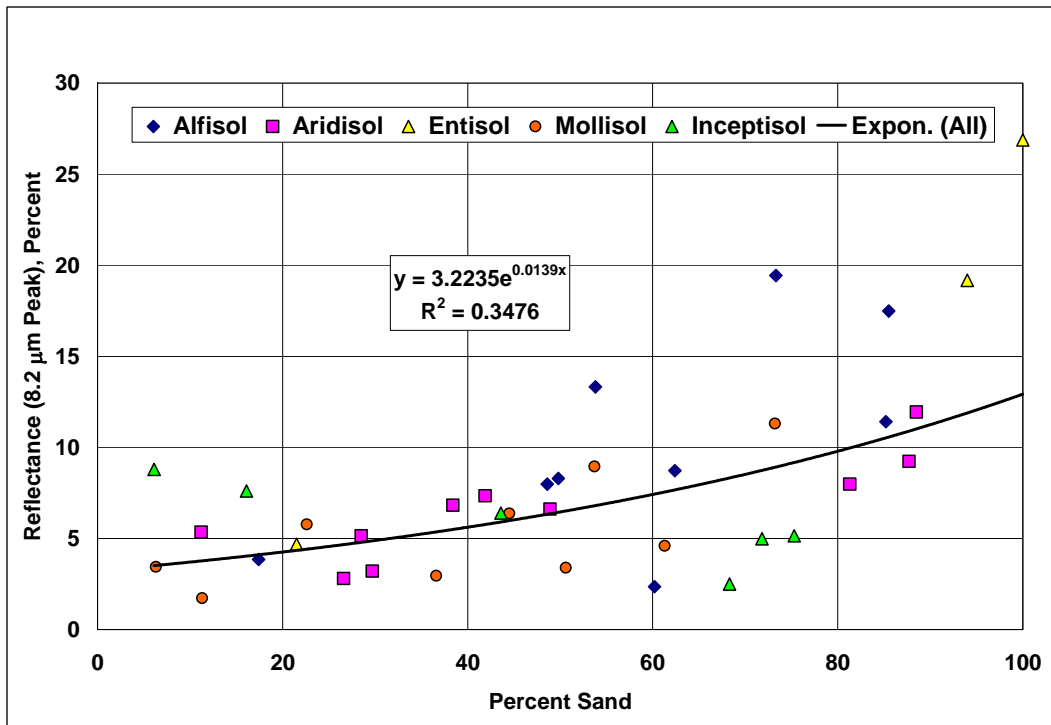


Figure 6. Percentage of peak reflectance at the 8.2-μm wavelength related to the percentage of sand in the soil.

Overall, the clay and silt plots show a nonlinear decrease in reflectance as the percentage of finer particles increases, a trend noted similarly by Salisbury and D'Aria (1992). From Appendix A, it can be seen that the mineralogy of the clay and silt fractions consists of nonreflective (nonquartz-bearing) minerals. Therefore, the increase in the presence of nonreflective fines within a composite soil reduces the presence of reflective quartz-bearing soil grains, creating an overall less reflective surface. Along the same line of reasoning, as the percentage of sand present in the soil increases, the reflectance also increases. These graphs agree with the known surface scattering effects in the 8- to 12- μm waveband, i.e., as particle size decreases, surface scattering increases, resulting in greater energy absorption, which translates to lower reflectance (Conel 1969). This is seen in the overall lower reflectance of the clay size particle fraction over that of the silt size fraction in Figures 4 and 5.

What is not accounted for in this data analysis is the study of any mineralogy that might otherwise dominate the quartz reflectance signature. Salisbury and D'Aria (1992) noted that gypsum, biotite, and feldspar can skew the reststrahlen feature by generating much larger reflectance signatures than those represented by the quartz-bearing minerals. Further investigation into the secondary mineralogy of the selected ASTER data may account for reflectance peaks far in excess of the noted trend lines.

Influence of impurities

Because the reststrahlen effect is dependent on the presence of quartz, the peak percentage of reflectance around the 8.2- μm wavelength and percentage of total quartz were used to compare the soil classes. It is instructive to look at the spectra of a pure quartz crystal versus other samples of quartz containing different impurities listed in Figure 7. Impurities in the crystal increase the percentage of peak reflectance 2 to 5 times, with smoky quartz (ts01b) showing the highest reflectance for these samples. The level of reflectance of composite soils at the 8.2- μm wavelength is generally less than 20% (Figure 6), which is closer to that of pure quartz (Figure 7) than it is to the impure varieties. This seems counterintuitive to the idea that the highest reflectance in the 8.2- μm reststrahlen band occurs only for pure quartz. This concept needs further study, as these types of impurities can occur anywhere and can significantly alter the measured reflectance.

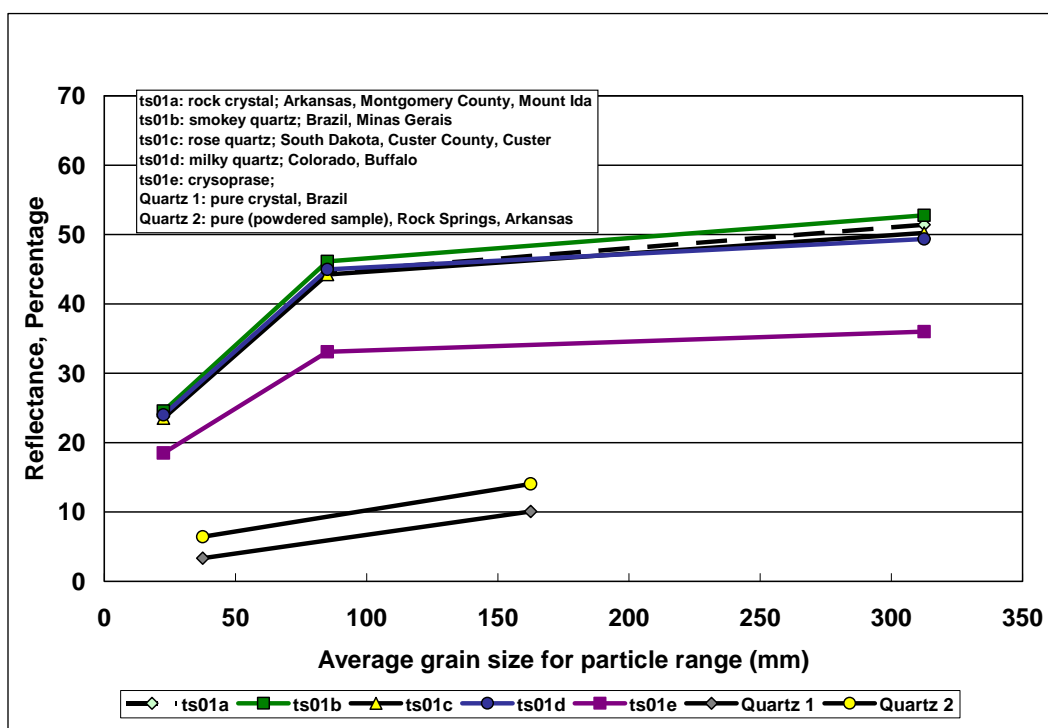


Figure 7. Percentage of peak reflectance at the 8.2- μm wavelength related to grain size for pure quartz and different quartz varieties (ASTER 1999).

Influence of quartz content

Figure 8 is a comparison of the reflectance of all five soil orders. Complete data were available for only one Entisol soil. There is a general trend for the reflectance to increase as the percentage of quartz in the soil increases. The coefficient of determination (R^2) of 0.63 is considered a strong correlation of the two datasets (x and y). The trend line fit was forced through the origin because, at 0% quartz, the reflectance is zero.

A linear regression fit to each of the individual soil classes, except Entisol, was also computed (Figures 9, 10, 11, and 12). The trend fits in the Alfisol and Mollisol plots were also forced to have a zero intercept. All of the individual soil orders have good individual coefficients of determination (R^2), lying between 0.56 and 0.74, as summarized in Table 2. The parameter x represents the percentage of quartz in a soil sample; y is the percentage of peak reflectance at the 8.2- μm quartz peak within the LWIR waveband. These relations allow prediction of an expected 8.2- μm quartz peak reflectance for a soil of given quartz percentage. This will define the expected

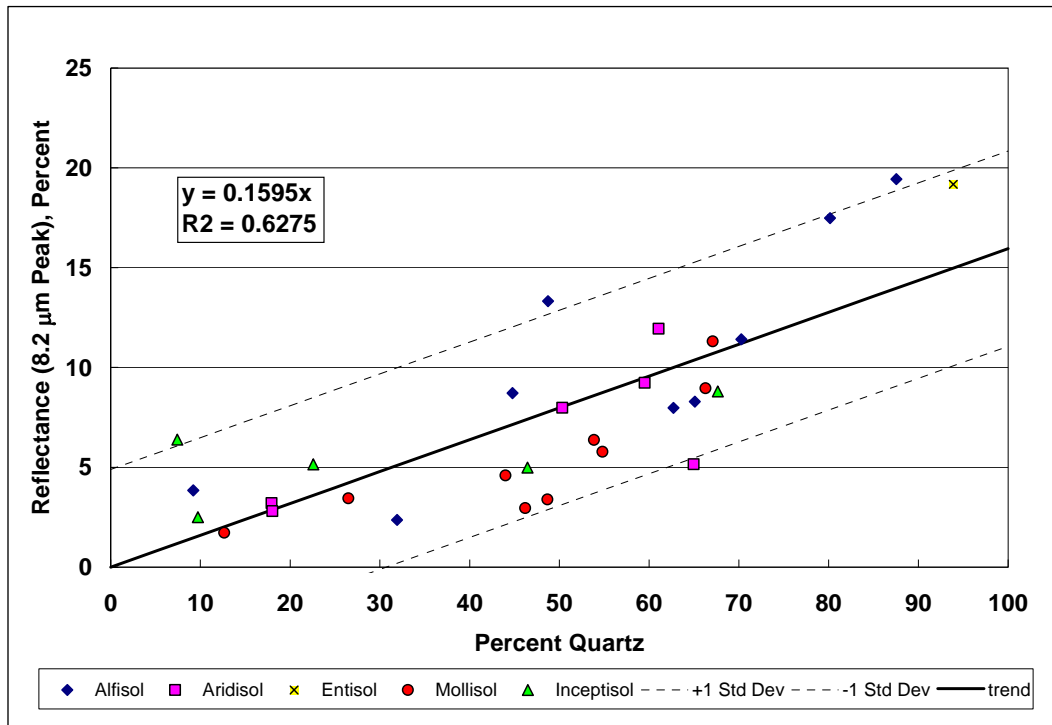


Figure 8. Linear fit to the combined ASTER soils data set. Percentage of peak reflectance at the 8.2-μm wavelength related to the percentage of quartz present in the soil sample.

Table 2. Relationships between percentage quartz content (x) to peak reflectance (y).

Soil	Equation	R ²
Combined (average)	$y = 0.1595x$	0.6275
Alfisol	$y = 0.1865x$	0.6831
Aridisol	$y = 0.1447x$	0.5566
Inceptisol	$y = 0.1372x$	0.7392
Mollisol	$y = 0.119x$	0.6667

disturbed reflectance for the native soil, allowing detection of disturbed soil or the presence of other foreign objects that should exhibit an increased reflectance signature.

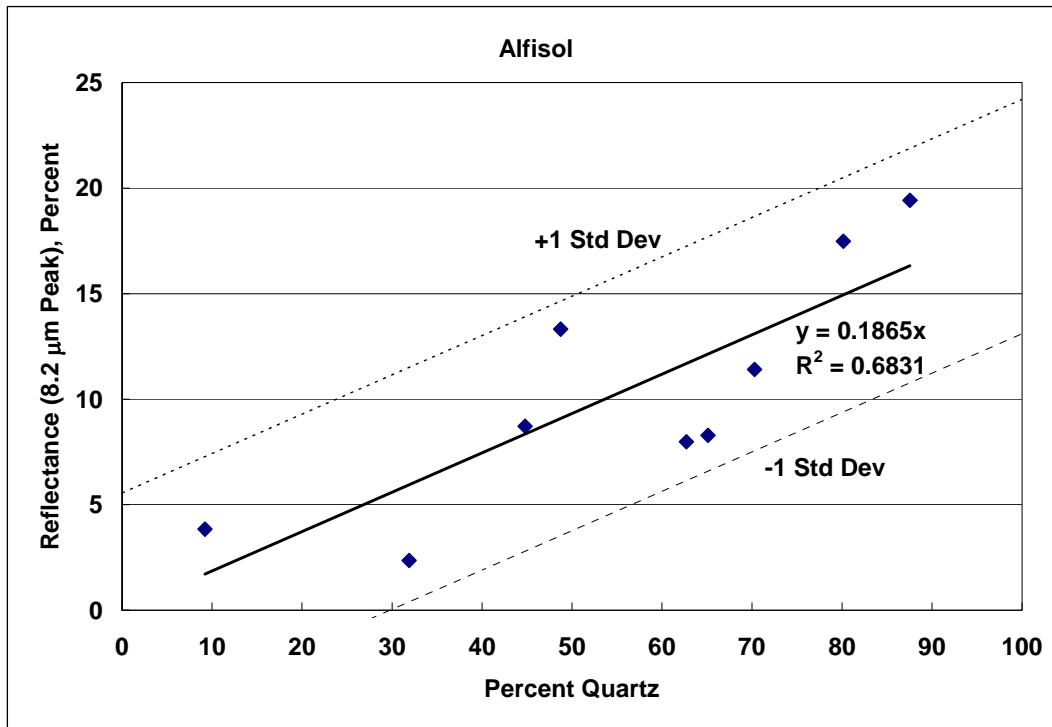


Figure 9. Linear fits of percentage of peak reflectance in Alfisols at the 8.2-μm wavelength related to the percentage of quartz present in the soil sample.

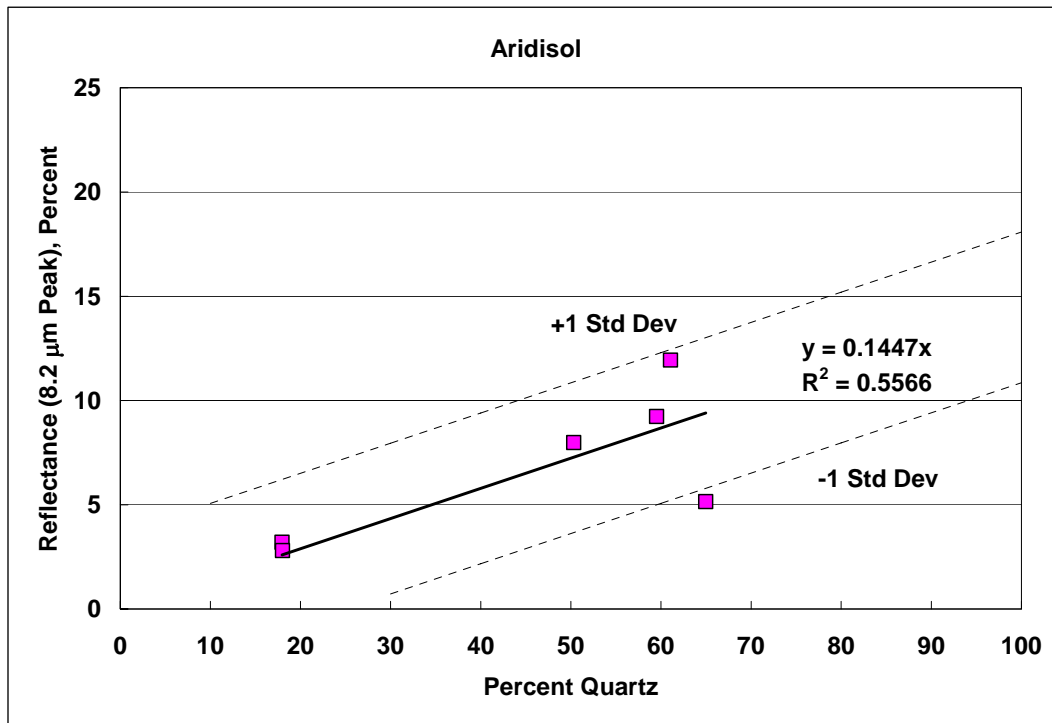


Figure 10. Linear fits of percentage of peak reflectance in Aridisols at the 8.2-μm wavelength related to the percentage of quartz present in the soil sample.

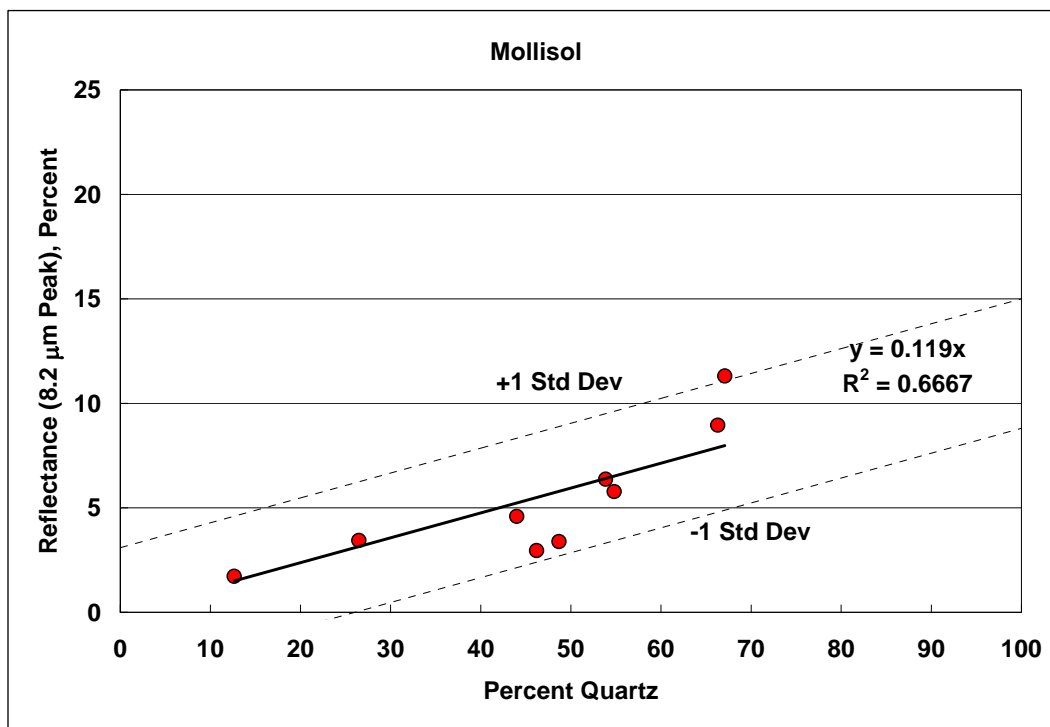


Figure 11. Linear fits of percentage of peak reflectance in Mollisols at the 8.2-μm wavelength related to the percentage of quartz present in the soil sample.

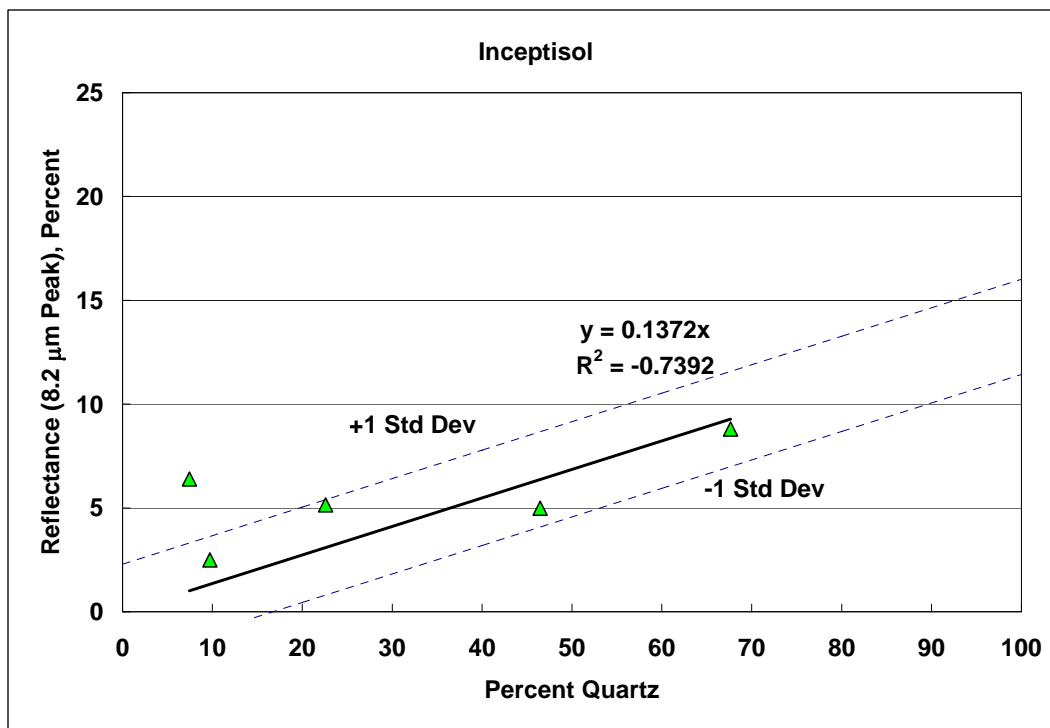


Figure 12. Linear fits of percentage of peak reflectance in Inceptisols at the 8.2-μm wavelength related to the percentage of quartz present in the soil sample.

3 Laboratory Study

Purpose

As shown in Chapter 2 of this report, grain size and mineralogical characteristics are among the factors that control the spectral reflectance of quartz. To explore the effects of grain size and mineral species on reflectance, laboratory experiments were conducted on three samples of natural quartz representing three polymorphic varieties. The influence on reflectance attributable to the influence of fine-grained clay was also investigated.

Approach

A laboratory Nicolet 750 FTIR spectrometer was used to investigate the reststrahlen effect (Figure 13). The FTIR spectrum provides a suitable estimate of the reststrahlen for a preliminary laboratory investigation of the effects of mineral speciation and grain size.



Figure 13. Nicolet 750 Fourier Transform Infrared Spectrometer.

Three samples of natural varieties of quartz (SiO_2) were selected for this investigation: a single-terminated quartz crystal from Hot Springs, AR; Dover chert; and Erwin quartzite from Tennessee. Each quartz sample is chemically similar (silicon dioxide with very minor impurities) but with differing crystalline lattice structures. The Hot Springs quartz crystal does not contain impurities and was formed by an igneous process. The Dover

chert is sedimentary, formed in a deep ocean environment; and the Erwin quartzite is metamorphic.

The Hot Springs quartz crystal was pulverized and sieved by standard sieving techniques to investigate the grain-size effect. The sample was divided into six distinct size fractions: that retained on the No. 16 (1180 μm), No. 20 (850 μm), No. 30 (600 μm), No. 40 (425 μm), No. 50 (300 μm) sieves and that passing the No. 50 sieve. The Dover chert and Erwin quartzite were similarly processed with only the amount retained and passing the No. 50 sieve used for analysis.

Influence of grain size

The primary focus of this effort was the investigation of the reststrahlen phenomenon using FTIR spectra as surrogates. The resulting data (as spectrographs of percentage of reflectance plotted against wavelength) were not normalized, but the effects observed approximate those attributed to the reststrahlen effect. For example, the first working assumption was that the FTIR spectra generated by differing grain-size fractions from a single type of quartz would differ. Based on the 50- μm split of material, the FTIR analysis agreed with other studies (Lyon 1964; Salisbury and Wald 1985) that the percentage of reflection is dependent on grain size (Figure 14). Further study on the material retained on the No. 50 sieve revealed an important finding. Reflectance actually decreased with increasing grain size in the coarse fraction (300- to 1180- μm range; Figure 15). This disagrees with the findings of Salisbury and Wald (1985) that quartz in the 250- μm range had a higher reflectance than quartz powders (0 to 74 μm) and of Conel (1969), who found increasing reflectance with grain size from 0- to 100- μm diameters. However, neither researcher studied the behavior of material exceeding 500 μm . The trend observed is nonlinear, nearly logarithmic, and the rate of reflectance increases as the grain size decreases (Figure 16).

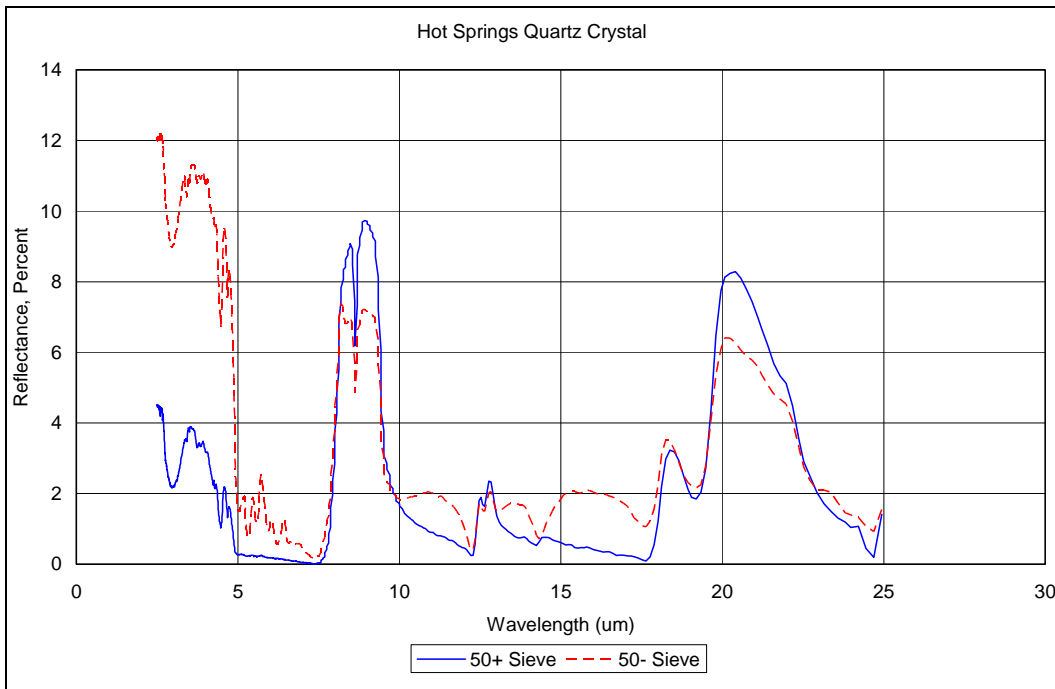


Figure 14. Spectra of coarser (50+) and finer (50-) grained quartz material.

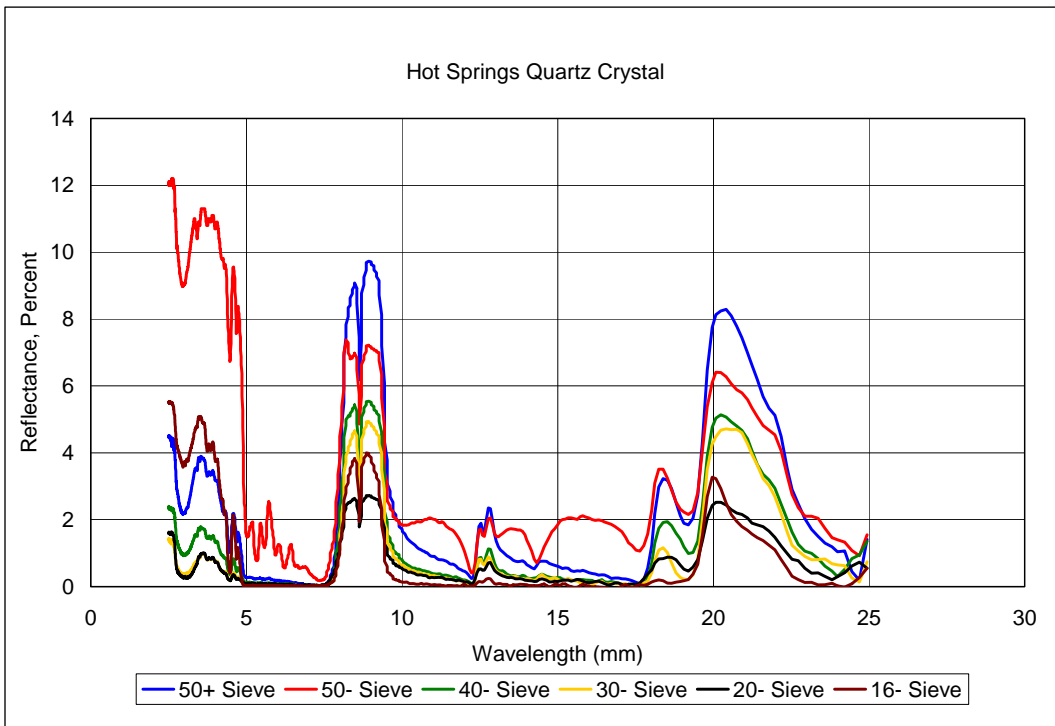


Figure 15. Reflectance for varying grain-size fractions for Hot Springs quartz.

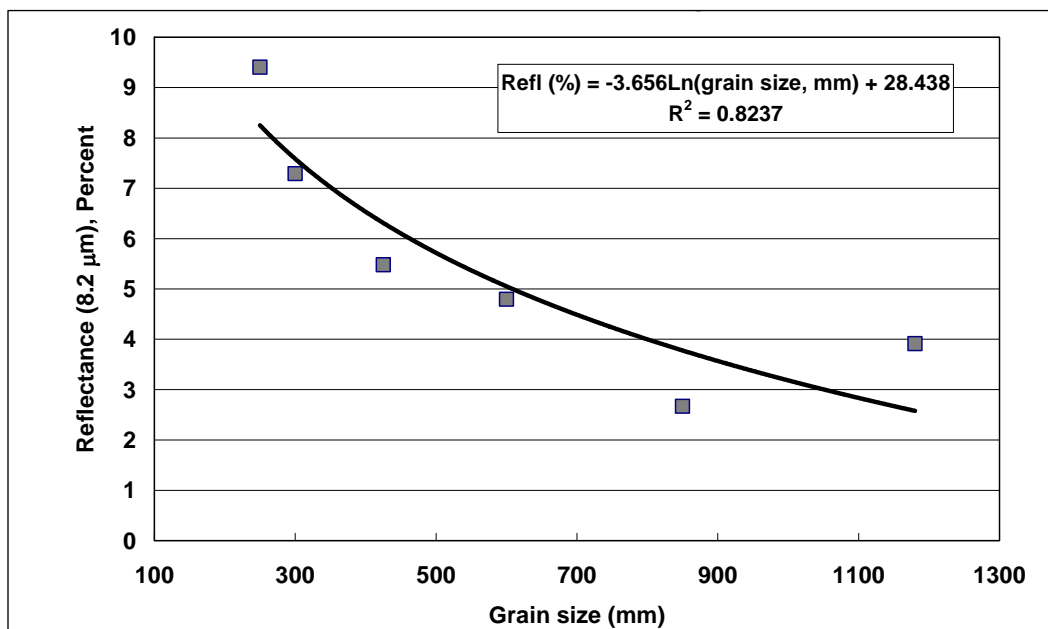


Figure 16. Trend of reflectance (y) for Hot Springs quartz with grain-size fraction (x).

Influence of quartz species

Also examined were two polymorphs of quartz, Dover chert and Erwin quartzite. The spectra from their fine fractions (minus No. 50) are compared to the spectrum for the same size fraction of Hot Springs quartz (Figure 17). Of the three samples, the pure quartz crystal exhibits the highest reflectance and the Dover chert the lowest. Because it forms by sedimentary rather than igneous processes, chert is poorly crystallized and considered to be cryptocrystalline relative to pure quartz. The FTIR spectra indicated that intensities vary from sample to sample according to the crystalline form of the mineral; that is, polymorphs of quartz will have very different reflectance peaks. The Hot Springs crystal has reflectance that is approximately 2.5 times greater than the Dover chert and about 1.5 times greater than the Erwin quartzite. This is a similar range of influence as seen due to quartz impurities shown in Figure 7.

Influence of fines content

Montmorillonite clay was used to study the change in reflectance attributable to the presence of fine particles. A USDA standard pure montmorillonite was used in the spectral analysis. A plot of its FTIR spectrum is shown as Figure 18. Montmorillonite was chosen because of its expansive characteristics and high ion exchange capacity. The ion

exchange capacity is a measure of how easily anions and cations can exchange within the crystal

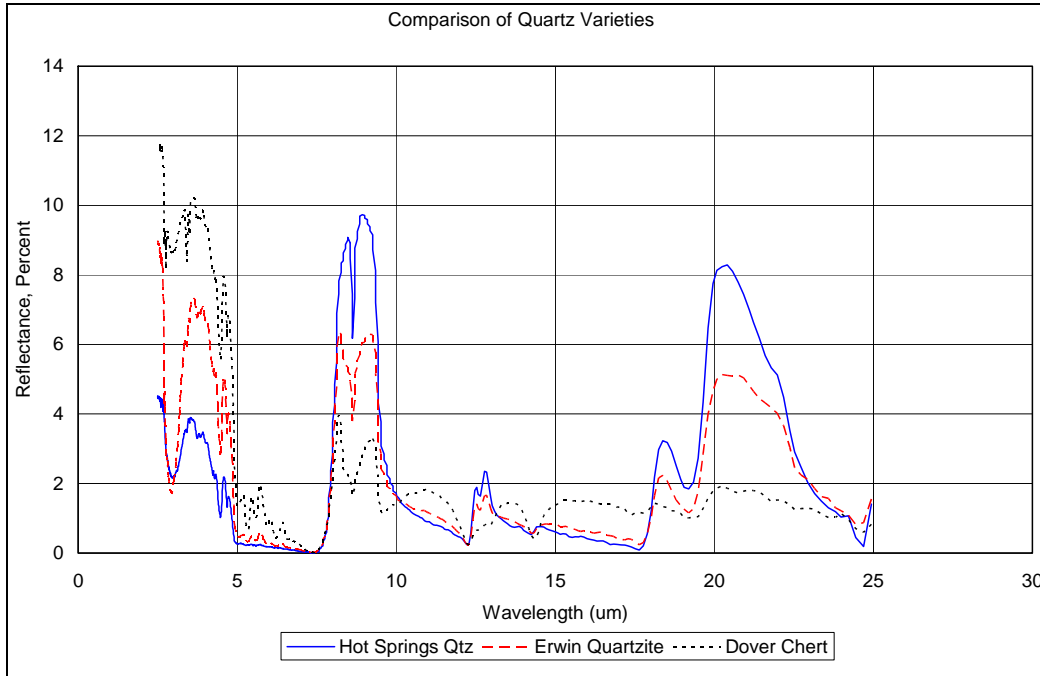


Figure 17. Comparison of spectra for three quartz species or three quartz species (coarser than No. 50 sieve).

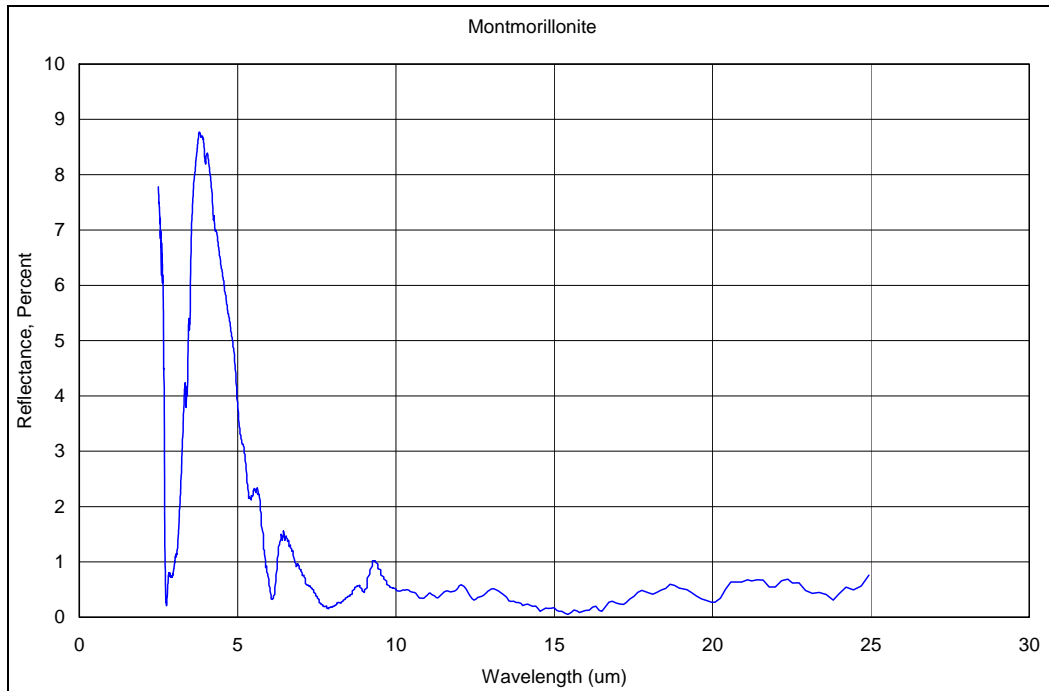


Figure 18. Spectrum of pure montmorillonite sample.

lattice of a mineral. FTIR spectra were measured for 50/50 dry blended mixtures by weight of montmorillonite/Hot Springs quartz, montmorillonite/Dover chert, and montmorillonite/Erwin quartzite (Figure 19). Spectra of these samples correlate well with what has been observed in other studies—that the addition of clay (as fines) reduces the overall reflectance signature in the 8.2- μm band.

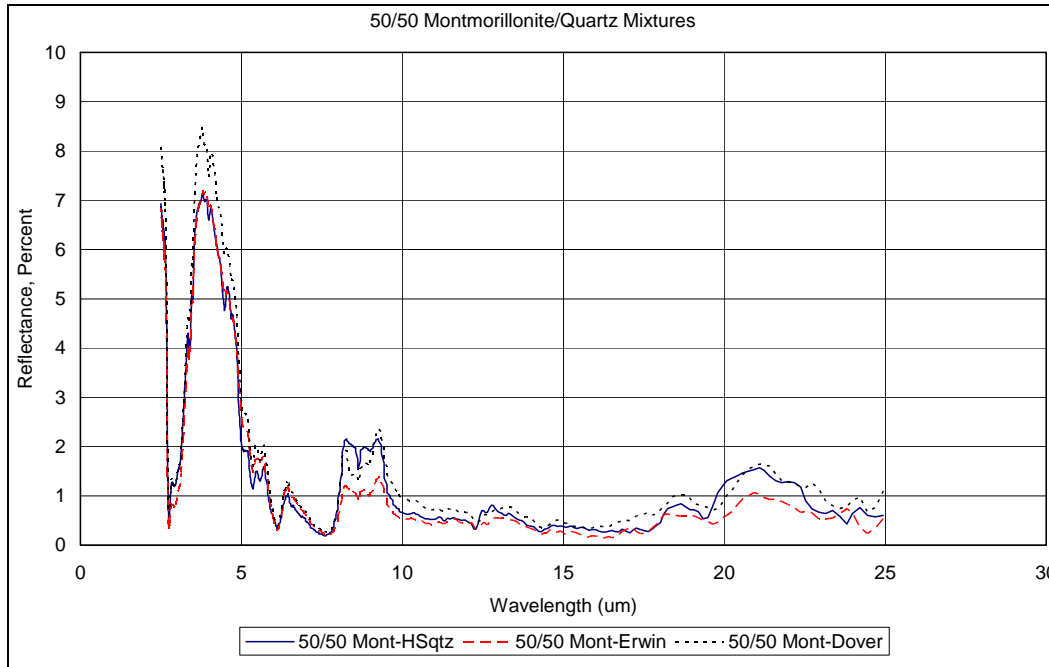


Figure 19. Spectra of montmorillonite mixed with the three quartz species (50/50).

It is possible that the degree of clay wetting and variable mineralogical structure that montmorillonite exhibits could influence its reflectance response. Attempts to develop time-series plots of moisture in a sample were unsuccessful because the chosen laboratory FTIR spectrometer is hypersensitive to atmospheric water vapor. Any addition of moisture to the montmorillonite/quartz mixtures resulted in erratic and “noisy” spectra and confounded meaningful interpretation. Moisture studies carried out by Salisbury and D’Aria (1992) showed that reflectance decreased with increasing moisture content.

4 Conclusions and Recommendations

Conclusions

The spectral response of quartz (the reststrahlen band) is a phenomenon of interest to countermine technologies because of suspected disruption in spectral signature from disturbed soil during emplacement of landmines in the subsurface. To determine the behavior of infrared spectral reflectance for varying soil orders, spectral and mineralogical data for 5 of the 12 major world soil orders were acquired from the ASTER spectral library maintained by the Jet Propulsion Laboratory.

Data relating the percentage of reflectance around the 8.2- μm quartz peak (reststrahlen band) to the percentage of quartz in a soil were used to fit linear equations to the combined soil data set and the individual soil orders. These relations allowed prediction of an expected 8.2- μm quartz peak reflectance for a soil of given quartz percentage with the average expression taken from Figure 8 as

$$\text{Reflectance (\%)} = 0.1595 * \text{Quartz content (\%)} \quad (1)$$

The reststrahlen response was also found to be dependent on the type of quartz and grain-size properties, which were an additional focus of this study. A laboratory Fourier transform infrared system was used to measure the spectral response of different forms of quartz, clays, and quartz-clay mixtures. The laboratory measurements revealed that different species of quartz exhibit different spectra, suggesting that the quartz reflectance response of a given soil type within the LWIR waveband will vary depending on its parent material. Specific quartz species can increase the measured peak reflectance shown in Equation 1 by as much as 2.5 times. Dry mixtures (50/50) of montmorillonite with crushed quartz reduced the reflectance by at least half, supporting the ASTER dataset which showed decreasing reflectance with increasing fines content. A quantitative relationship may describe the effect of fines on the spectral response.

Grain-size fraction plays an important role in determining the magnitude of reflectance. For a pure quartz sample, as the grain size decreased from particle diameters of 1180 μm to less than 300 μm , the FTIR reflectance

increased according to a logarithmic relationship given in Equation 2. Previous work suggested that reflectance increases with increasing grain size; however, this relationship has been demonstrated only with soil diameters of less than 500- μm fractions and usually less than 100 μm .

$$\text{Reflectance (\%)} = -3.656 \ln(\text{Grain size in } \mu\text{m}) + 28.438 \quad (2)$$

The findings presented in this report allow a coarse approximation of the expected disturbed reststrahlen signatures for native soil given knowledge of grain size and mineralogy. The correlations in this report do not include gravel-sized aggregates that are often present in natural soils. Therefore, some deviation in the spectral response is expected based on the presence of larger grains. The predictive equations are a step toward improving techniques to detect locations of disturbed soil or buried objects based on differences in reststrahlen signature.

Recommendations

An important finding of the laboratory investigation is that polymorphs of quartz produce different infrared spectra (Figure 8). The percentage of reflectance was different for each mineral, indicating the polymorphs of quartz and other minerals with polymorphs will have different infrared spectra. Although the polymorphs of quartz studied exhibit distinct reflectance intensities near 8.2 μm , when fines (montmorillonite) were added to the samples, the difference in spectral response was greatly reduced. Further laboratory studies should be conducted to determine if there is a quantitative relationship between reflectance intensity and the quantity and chemical composition of the fine fraction.

Future studies should evaluate the spectral response of the coarser grain-size fraction of the quartz materials (exceeding 1200 μm) to account for the presence of larger aggregates in native soils. Grain size coupled with quartz content will account for many of the corrections necessary to predict field reflectance for undisturbed soils.

To better characterize field reflectance values for native soils, environmental effects must be included in future FTIR studies focusing on moisture and density variables. An analysis of these variables along with grain-size distribution and quantitative mineralogy of each soil studied at successive time increments during a test will allow a better understanding of the effects of the weather effects and elapsed time on soil-reflectance

properties. Relationships can then be developed to estimate the soil reflectance within the reststrahlen band for a variety of soil types under different meteorological conditions over a short time period, simulating typical mission execution in the field to identify disturbed soil (Koh et al. 2006).

References

- ASTER (Advanced Spaceborne Thermal Emission and Reflection) Spectral Library. 1999. Pasadena, CA: Jet Propulsion Laboratory, California Institute of Technology.
- Broekmans, M. A. T. M. 2004. Structural properties of quartz and their potential role for ASR. *Materials Characterizations* 53:129–140.
- Conel, J. E. 1969. Infrared emissivities of silicates: Experimental results and a cloudy atmosphere model of spectral emission from condensed particulate mediums. *Journal of Geophysical Research* 74(6):1614–1634.
- ERIM International, Inc. 1999a. *Mine spectral signature collection and data archive*. Report No. 10012200-15-T. Ann Arbor, MI.
- _____. 1999b. *Spectral mine detection study*. Report No. 10012200-17-F. Ann Arbor, MI.
- Hamilton, V. E. 2003. Constraints on the composition and particle size of high albedo regions on Mars. In *Sixth International Conference on Mars*.
- Hook, S. J., and A. B. Kahle. 1996. The micro Fourier transform interferometer (μ FTIR)—A new field spectrometer for acquisition of infrared data on natural surfaces. *Remote Sensing Environment* 56:172–181.
- Kelch, D. J., D. A. Fatora, R. K. Hill, K. Krause, P. R. Lind, E. Siler, B. L. Sink, and D. Sira. 1999. Spectral phenomenon for detection of disturbed soil. In *ISSSR '99*, 31 Oct–4 Nov, Las Vegas, NV.
- Koh, G., E. M. Winter, and M. A. Schatten. 2006. Rainfall degradation of LWIR disturbed soil signature. In *Proceedings, Detection and Remediation Technologies for Mines and Minelike Targets XI*, 6217 I:62170G. Bellingham, WA: SPIE—The International Society for Optical Engineering.
- Korte, E. H., and A. Röseler. 2005. Infrared reststrahlen revisited: commonly disregarded optical details related to $n < 1$. *Analytical and Bioanalytical Chemistry* 382:1987–1992.
- Lyon, R. J. P. 1964. *Evaluation of infrared spectrophotometry for compositional analysis of lunar and planetary soils; Part 2: Rough and powdered surfaces*. Report NASA CR-100.
- MTL Systems, Inc. 1999. *Hyperspectral mine detection phenomenology study*. Beaver-creek, OH.
- Nicodemus, F. E. 1965. Directional reflectance and emissivity of an opaque surface. *Applied Optics* 4:767–773.
- SAIC. 1998. *Hyperspectral measurements for mine detection (Draft)*. Arlington, VA.

- Salisbury, J. W., and D. M. D'Aria. 1992. Infrared (8–14 micron) remote sensing of soil particle size. *Remote Sensing of Environment* 42:147–165.
- Salisbury, J. W., and A. Wald. 1985. The effect of particle size and porosity on spectral contrast in the mid-infrared. *ICARUS* 64:586–588.
- Salisbury, J. W., B. Hapke, and J. S. Eastes. 1987. Usefulness of weak bands in the midinfrared remote sensing of particulate planetary surfaces. *Journal of Geophysical Resources* 92:702–710.
- U.S. Department of Agriculture, Natural Resources Conservation Service (USDA–NRCS). Soil Survey Division Staff, Soil Conservation Service. 1993. *Soil survey manual*. USDA Handbook 18. ftp://ftp-fc.sc.egov.usda.gov/NSSC/Soil_Taxonomy/tax.pdf.
- _____. 1999. *Soil taxonomy; A basic system of soil classification for making and interpreting soil surveys*. 2d ed. Agriculture Handbook No. 436.
- _____. 2002. *Field book for describing and sampling soils, Version 2.0*, ed. P. J. Schoeneberger, D. A. Wysocki, E. C. Benham, and W. D. Broderson. Lincoln, NE: National Soil Survey Center.

Appendix A: Summary of Soil Data

This appendix summarizes the soil information obtained from the ASTER Spectra Soil Library database (1999), including soil order, grain size information (percentages of sand, silt and clay size particles), and mineralogy of the clay-size fraction and silt/sand-size fraction, labeled “clay” and “coarse,” respectively.

Mineral abbreviations used in Table A1 are as follows:

Kaol = kaolinite

Mont = montmorillonite

Ill/Musc = illite/muscovite

Verm = vermiculite

K-Spar = potassium feldspar

Plag = plagioclase

Table A1. Summary of soil data (ASTER Spectral Library).

Order	Description	Organic Carbon, %	Size Fraction			Clay Mineralogy					Coarse Mineralogy				
			Clay, %	Silt, %	Sand, %	Kaol	Mont	Ill/Musc	Verm	Mica	Quartz, %	K-Spar, %	Plag, %	Glass, %	Description
Alfisol	pale brown silty loam	2.35	7.9	74.7	17.4	x			x	x	10		x	50	40% glass aggregate; trace tourmaline
Alfisol	reddish brown fine sandy loam	1.3	20.1	26.1	53.8	x	x			x	61	19	4		12% chalcedony; 3% clay-coated quartz; traces of others
Alfisol	reddish brown fine sandy loam	0.16	7.3	7.7	85.5	x	x			x	86	12	x		traces of others
Alfisol	brown sandy loam	0.71	12.2	25.4	62.4	x	x			x	51	31	2		7% biotite; 6% opaque; 1% hornblende, traces of others
Alfisol	brown to dark brown gravelly loam	8.54	4.2	36.5	60.2		x				33		7	9	39% weathered aggregate; 4% tourmaline; 4% glass-coated Grains
Alfisol	brown loamy fine sand	0.86	6.3	8.5	85.2	x			x	x	75	20	4		3% tourmaline; trace muscovite, microcline, opaque
Alfisol	brown fine sandy loam	0.76	7	43.2	49.8	x	x			x	70	17	x	4	1% each muscovite, biotite, opaque, amphibole, zircon; trace other
Alfisol	brown fine sandy loam	1.15	6.4	45	48.6	x	x			x	67	17	1	7	3% opaque; 2% amphibole; 1% biotite; traces of others
Alfisol	dark reddish brown fine sandy loam	1.44	8.8	17.9	73.3	x				x	96				4% iron oxides; traces of others
Aridisol	dark brown interior moist clay loam	1.03	11.1	50.5	38.4										15.5% CaCO ₃ ; 3.5% CaSO ₄

Order	Description	Organic Carbon, %	Size Fraction			Clay Mineralogy					Coarse Mineralogy					
			Clay, %	Silt, %	Sand, %	Kaol	Mont	Ill/Musc	Verm	Mica	Quartz, %	K-Spar, %	Plag, %	Glass, %	Description	
Aridisol	light yellowish brown interior dry gravelly loam	0.5	10.7	40.4	48.9										21% CaCO3	
Aridisol	brown to brownish yellow dry gravelly silt loam	0.47	16.4	41.7	41.9										7% CaCO3; 18% CaSO4	
Aridisol	light yellowish brown loam	1.02	18.1	70.7	11.2										20% CaCO3	
Aridisol	brown silty loam	0.89	7.2	64.3	28.5						70	trace	3	10	8% glass aggregate; 4% tourmaline; 3% muscovite; 2% glass-coated grains	
Aridisol	light yellowish brown clay	0.68	51.5	18.8	29.7					x	37	10	trace		36% carb-aggregate; 4% opaque; 3% hornblende; 2% biotite; 1% calcite; 5% other; traces other	
Aridisol	light yellowish brown loamy sand	0.13	4	8.3	87.7						62	16	2		10% other; 4% opaque; 3% biotite; 2% hornblende; 1% zircon; trace other	
Aridisol	brown gravelly sandy loam	0.1	3.2	15.5	81.3	x	x				x	52	17	1	16% other; 7% opaque; 3% biotite; 3% hornblende; 1% goethite; 1% zircon; trace other	
Aridisol	dark yellowish brown silty clay	0.4	58.1	15.3	26.6	x	x				x	43	12	2	trace	25% biotite; 9% hornblende; 5% other; 3% opaque; 2% zircon; trace other
Aridisol	very dark grayish brown loamy sand	0.51	4.6	6.9	88.5							64	2	2		21% feldspar; 2% opaque; 7% other; trace other

Order	Description	Organic Carbon, %	Size Fraction			Clay Mineralogy					Coarse Mineralogy					
			Clay, %	Silt, %	Sand, %	Kaol	Mont	Ill/Musc	Verm	Mica	Quartz, %	K-Spar, %	Plag, %	Glass, %	Description	
Aridisol	red-orange sandy soil					5%		9%				79				
Aridisol	red-orange sandy soil					6%	x	16%				61				12% smectite
Aridisol	grey calcareous silty soil					x		19%				49				22% smectite (chlorite + montmorillonite); 7% calcite
Aridisol	grey calcareous silty soil					x	x	x								Fe Chlorite;
Entisol	fluvial deposit	see comment						trace				59				20% smectite; grain size analysis of fraction finer than 2 mm indicates 35% finer than 20 micrometer (12% finer than 5 micrometer)
Entisol	red-orange sandy loam/alluvium	see comment				8%	x	10%				72				7% smectite; 47% finer than 20 µm (22% finer than 5 µm)
Entisol	sandy loam/alluvium	see comment	x			12%		11%				63				10% smectite; 57% finer than 20 µm (24% finer than 5 µm)
Entisol	alluvial sand	see comment				x						94				8% finer than 20 um (5% finer than 5 µm)
Entisol	red-orange sandy loam	see comment				13%	x	15%				58				11% smectite; 52% finer than 20 µm (23% finer than 5 µm)
Entisol	red-orange sandy loam	see comment				6%		9%				76				4% smectite; 34% finer than 20 µm (15% finer than 5 µm)
Entisol	red-orange sandy loam	see comment				6%		11%				67				13% smectite; 38% finer than 20 µm (16% finer than 5 µm)

Order	Description	Organic Carbon, %	Size Fraction			Clay Mineralogy					Coarse Mineralogy					
			Clay, %	Silt, %	Sand, %	Kaol	Mont	Ill/Musc	Verm	Mica	Quartz, %	K-Spar, %	Plag, %	Glass, %	Description	
Inceptisol	pale brown dry silty clay loam	0.95	36.5	47.4	16.1	NA					NA				29% CaCO3	
Inceptisol	very dark grayish brown silty loam	3.8	12.9	84.1	6.1	x	x			x	3%	75	14		3% opaque; 1% each tourmaline, plant opal, zircon, amphibole, other weathered materials	
Inceptisol	dark brown fine sandy loam	3.41	5.9	18.8	75.3	x				x	x	24	2	16	34% biotite; 10% muscovite; 8% garnet; 1% each epidote, rutile, pyroxene, zircon, opaque, weathered aggregate;	
Inceptisol	brown to dark brown gravelly fine sandy loam	5.43	2.7	29	68.3	NA						10		7	40% weathered aggregate; 24% glass-coated grains; 19% glass aggregate; 1% tourmaline;	
Inceptisol	gray/dark brown extremely stony coarse sand	6.18	7.1	21.1	71.8	x	x				x	50	7	1	trace	20% muscovite; 9% other; 7% biotite; 5% opaque; 1% chlorite; trace hematite, pyroxene, zircon, calcite, hornblende;
Inceptisol	dark yellowish brown micaceous loam	0.96	25.7	30.7	43.6	x					x	x	10	2		67% biotite; 17% muscovite; 3% goethite; 2% opaque; trace garnet, plant opal, tourmaline, chlorite, rutile, zircon;
Inceptisol	brown sandy loam	NA				NA						50		trace	24% muscovite; 17% biotite; 3% other; 2% garnet; 1% opaque; 1% hornblende; trace rutile, tourmaline, chlorite, zircon;	

Order	Description	Organic Carbon, %	Size Fraction			Clay Mineralogy					Coarse Mineralogy					
			Clay, %	Silt, %	Sand, %	Kaol	Mont	Ill/Musc	Verm	Mica	Quartz, %	K-Spar, %	Plag, %	Glass, %	Description	
Mollisol	grayish brown loam	2.49	12	26.7	61.3	trace	x				50	12	6	12	8% glass aggregate; 4% hornblende; 2% opaque; 1% each zircon, carb-aggregate, other, epidote, biotite, calcite; trace muscovite	
Mollisol	black loam	6.64	17.5	45.9	36.6	trace	x			trace	trace	56		2	6	30% glass aggregate; 6.4% tourmaline;
Mollisol	dark grayish brown silty loam	2.29	30.3	63.4	6.3	trace	x			trace	10%	38	11	15	7	8% plant opal; 4% opaque; 3% pyroxene; 2% hornblende; 1% weathered materials; trace tourmaline
Mollisol	gray silty clay	1.88	25.6	63.1	11.3	x	x				x	17		4	trace	calcite; 78% other weathered materials; 1% tourmaline; trace muscovite
Mollisol	very dark grayish brown loam	2.87	17.5	31.9	50.6	x	x				x	59	25	2	1	5% opaque; 3% other; 2% pyroxene; 1% each goethite, weathered aggregate, zircon, hematite; trace biotite and plant opal;
Mollisol	very dark grayish brown loam	1.06	13.9	32.4	53.7	x					x	x	77	16	trace	goethite; 3% resistant aggregate; 1% other; 1% hornblende; trace zircon, opaque, amphibole, pyroxene, biotite;
Mollisol	brown to dark brown sandy loam	0.61	8.1	18.7	73.2	x					x	x	73	15		goethite; 5% weathered aggregate; 4% resistant aggregate; 2% opaque; 1% other; 1% zircon; traces biotite, amphibole, garnet, chlorite;

Order	Description	Organic Carbon, %	Size Fraction			Clay Mineralogy					Coarse Mineralogy				
			Clay, %	Silt, %	Sand, %	Kaol	Mont	Ill/Musc	Verm	Mica	Quartz, %	K-Spar, %	Plag, %	Glass, %	Description
Mollisol	very dark grayish brown silty loam	2.22	22.8	54.6	22.6	x	x			x	71	1	1	4	11% feldspar; 1% each biotite, plant opal, iron oxides, glass aggregate, glass-coated grains, muscovite; 2% other; 3% weathered aggregate; trace hornblende, zircon, apatite, pyroxene, garnet
Mollisol	very dark grayish brown loam	1.11	14.5	41	44.5	x	x			x	63	2	1	1	chlorite; 18% feldspar; 5% other; 4% weathered aggregate; 2% opaque; 1% each glass aggregate, biotite, hornblende; trace zircon, tourmaline, glass-coated grains, plant opal, garnet, carb-aggregate, muscovite;

REPORT DOCUMENTATION PAGE

Form Approved
OMB No. 0704-0188

Public reporting burden for this collection of information is estimated to average 1 hour per response, including the time for reviewing instructions, searching existing data sources, gathering and maintaining the data needed, and completing and reviewing this collection of information. Send comments regarding this burden estimate or any other aspect of this collection of information, including suggestions for reducing this burden to Department of Defense, Washington Headquarters Services, Directorate for Information Operations and Reports (0704-0188), 1215 Jefferson Davis Highway, Suite 1204, Arlington, VA 22202-4302. Respondents should be aware that notwithstanding any other provision of law, no person shall be subject to any penalty for failing to comply with a collection of information if it does not display a currently valid OMB control number. **PLEASE DO NOT RETURN YOUR FORM TO THE ABOVE ADDRESS.**

1. REPORT DATE (DD-MM-YYYY) August 2009		2. REPORT TYPE Final report		3. DATES COVERED (From - To)	
4. TITLE AND SUBTITLE Analysis of Long Wave Infrared (LWIR) Soil Data to Predict Reflectance Response				5a. CONTRACT NUMBER	
				5b. GRANT NUMBER	
				5c. PROGRAM ELEMENT NUMBER	
6. AUTHOR(S) Janet E. Simms, Ernest S. Berney IV, Danny W. Harrelson, Maureen K. Corcoran, and Ray M. Castellane				5d. PROJECT NUMBER	
				5e. TASK NUMBER	
				5f. WORK UNIT NUMBER	
7. PERFORMING ORGANIZATION NAME(S) AND ADDRESS(ES) U.S. Army Engineer Research and Development Center Geotechnical and Structures Laboratory 3909 Halls Ferry Road Vicksburg, MS 39180-6199				8. PERFORMING ORGANIZATION REPORT NUMBER ERDC/GSL TR-09-25	
9. SPONSORING / MONITORING AGENCY NAME(S) AND ADDRESS(ES) Headquarters, U.S. Army Corps of Engineers Washington, DC 20314-1000				10. SPONSOR/MONITOR'S ACRONYM(S)	
				11. SPONSOR/MONITOR'S REPORT NUMBER(S)	
12. DISTRIBUTION / AVAILABILITY STATEMENT Approved for public release; distribution is unlimited.					
13. SUPPLEMENTARY NOTES					
14. ABSTRACT The spectral response of quartz is a phenomenon of interest to countermine technologies because of suspected disruption in spectral signature from disturbed soil during emplacement of landmines in the subsurface. The research was divided into two studies: data analysis using spectral information from the Advanced Spaceborne Thermal Emission and Reflection (ASTER) spectral library and a laboratory study using a Fourier transform infrared (FTIR) spectrometer. Spectral and mineralogical data for five major soil orders (Alfisol, Aridisol, Entisol, Mollisol, and Inceptisol) were acquired from the spectral library. Using these data, the relationship of the percentage of reflectance around the 8.2- μ m quartz peak to the percentage of quartz in a soil was used to develop a linear regression model. The equations from this model predict the expected quartz peak (Continued)					
15. SUBJECT TERMS					
Clay		Quartz		Sand	
Emissivity		Reflectance		Silt	
Long wave infrared		Reststrahlen		Soil	
16. SECURITY CLASSIFICATION OF:			17. LIMITATION OF ABSTRACT	18. NUMBER OF PAGES	19a. NAME OF RESPONSIBLE PERSON
a. REPORT	b. ABSTRACT	c. THIS PAGE			19b. TELEPHONE NUMBER (include area code)
UNCLASSIFIED	UNCLASSIFIED	UNCLASSIFIED		42	

14. ABSTRACT (Concluded)

reflectance for a soil of given quartz percentage. The predictive equations determined from the ASTER database can be modified based on quartz species and grain size to enable better prediction of expected reflectance from natural soils.

The FTIR system was used to measure the spectral response of different forms of quartz, clays, and quartz-clay mixtures. The spectral results revealed that different species of quartz exhibit different reflectance spectra, suggesting that the quartz reflectance response of a given soil type will vary depending on its impurities and depositional history. Grain-size fraction plays an important role in influencing the magnitude of reflectance. From the pure quartz studied, as grain size decreased from particle diameters of 1180 μm to less than 300 μm , FTIR reflectance increased according to a logarithmic relationship.